1977

Comparative analysis of the analytical capabilities of coherent anti-Stokes Raman Spectography relative to Raman scattering amd absorption spectrosopy

Tolles, W. M.

Society for Applied Spectroscopy

A Comparative Analysis of the Analytical Capabilities of Coherent Anti-Stokes Raman Spectroscopy (CARS) Relative to Raman Scattering and Absorption Spectroscopy

W. M. TOLLES and R. D. TURNER*

Department of Physics and Chemistry, Naval Postgraduate School, Monterey, California 93940

The performance capabilities of coherent anti-stokes Raman spectroscopy (CARS) relative to incoherent Raman scattering and absorption spectroscopy are considered for gases. Four gases are considered for model calculations: hydrogen, nitrogen, oxygen, and carbon monoxide. The signal/noise ratio is estimated for these molecules under a number of assumed experimental conditions. The signal/noise ratios for CARS and Raman scattering scale quite differently with partial pressure and temperature. CARS offers distinct advantages when detecting a major component of a gas mixture at total pressures of considerably less than 1 atm pressure. Raman scattering offers 1 to 2 orders of magnitude greater sensitivity for a signal/noise ratio of unity when detecting a minor component of a gaseous mixture at 1 atm total pressure. These model calculations should be of use when a specific experimental method is to be chosen for spectroscopic examination.

Index Headings: **Coherent anti-Stokes Raman spectroscopy (CARS); Raman spectroscopy.**

INTRODUCTION

Coherent anti-Stokes Raman spectroscopy (CARS) has recently generated considerable interest as a tool for spectroscopic analysis. The method has been applied to the observations of resonances in solids,[1–4] liquids,[4–9] and gases.[10–16] A review has appeared recently.[17] The most attractive aspect of CARS as a spectroscopic tool is that much higher conversion efficiencies to anti-Stokes signals are possible relative to similar efficiencies by incoherent Raman scattering. The use of Raman scattering for combustion studies is well documented.[18–21] The interference due to fluorescent particles in the flame has been noted[22] as a limitation in the sensitivity achieved by Raman scattering. Spatial discrimination from luminescent samples is afforded by the collimated nature of the CARS spectral signal.

A careful analysis of the analytical capabilities of CARS relative to other analytical methods has not yet appeared in the literature. Such an analysis, applied to several simple molecules, is presented here. Included in this analysis are absorption spectroscopy and ordinary Raman scattering. Absorption spectroscopy is included because typically the dominant noise source with this technique is due to amplitude jitter of the radiation source. It is found that under many situations the limiting sensitivity of CARS is due to this same mechanism. Raman scattering is included because information gathered by CARS is similar to that gathered by Raman scattering.

The pressure of a sample which gives a specific signal/noise ratio is calculated for a series of assumed experimental conditions. The parameters assumed for these calculations represent those countered in present day experimental devices. Electronic resonance enhancement has been found to give orders of magnitude improvement in signal/noise ratios in liquids.[5] For many diatomic species in gases this advantage cannot be realized and is not considered in this analysis.

The calculations presented serve to give perspective to the capabilities and limitations of CARS relative to the problems to which it may be applied.

I. ESTIMATION OF SIGNAL/NOISE RATIOS

In order to make a comparative analysis involving various spectroscopic methods, a parameter such as signal/noise ratio is commonly desired. The signal/noise ratio referred to in this paper refers to the signal level due to the presence of a spectral resonance relative to the noise level present from a variety of sources which interferes with the determination of the magnitude of the resonance. In some cases the signal level may be a small change in the magnitude of a background light source, such as with absorption spectroscopy. In other cases, such as with Raman scattering, the signal level may be the only light received by the apparatus.

The general relationship for a signal/noise ratio (S/N) which will be used is

$$\mathrm{S/N} = \frac{P_s}{\left[\sum_i P_{Ni}^2\right]^{1/2}} \tag{1}$$

where P_s is the magnitude of the power due to the signal and P_{Ni} is the noise power contributed from the ith source of noise considered. This relation assumes that the noise contributed from the various sources is uncorrelated. The magnitudes of P_s and P_{Ni} are presented below for each of several spectroscopic methods commonly utilized. For each of the formulas given the signal and noise power are specified for a single pulse.

A. P_s for Absorption. For a single pass through a

Received 14 May 1976; revision received 15 September 1976.

* Lieutenant, U. S. Navy.

sample of length L, the magnitude of P_s corresponds to the change in power reaching the detector when the frequency of the electromagnetic radiation is tuned over the spectral transition. This is equal to

$$P_s(\text{ABS}) = P_o(1 - e^{-N\sigma_{\text{ABS}}L})\eta_o\eta_d \cong P_o N\sigma_{ABS} L\eta_o\eta_d \quad (2)$$

where P_o is the power from the radiation source, N is the number density of the absorbing species, σ_{ABS} is the absorption cross-section, and η_o and η_d are the efficiencies of the optics and detector, respectively. The approximation is valid when $N\sigma_{\text{ABS}}L \ll 1$, which is usually the case for signals near the detectability limit. This relationship also assumes that extinction due to other absorbers or scattering species is negligible.

In general, for a Lorentzian line shape,

$$\sigma_{\text{ABS}} = \frac{2SkT}{\pi\gamma} \quad (3)$$

where S is the integrated absorption coefficient over a spectral absorption, k is the Boltzmann constant, T is temperature, and γ is the full line width measured at half-maximum. Values of S for a number of spectral absorptions have been tabulated.[23] Combining the last two equations and assuming ideal gas law behavior,

$$P_s(\text{ABS}) \cong P_o\left(\frac{2}{\pi}\frac{PSL}{\gamma}\right)\eta_o\eta_d \quad (4)$$

where P is the pressure of the absorbing species.

B. P_s for Raman Backscatter Measurements. For a backscattering (LIDAR) arrangement in which the scattered radiation reaches the detector from an effective sample length of $L = c\tau/2$[24] for a pulse duration of τ,

$$P_s(\text{BS}) = P_o N\left(\frac{d\sigma}{d\Omega}\right) L\frac{A}{R^2}\eta_o\eta_d = P_o N\left(\frac{d\sigma}{d\Omega}\right)\frac{Ac\tau}{2R^2}\eta_o\eta_d \quad (5)$$

where P_o is the power of the incident beam, as before, $d\sigma/d\Omega$ is the differential Raman scattering cross-section, A is the area of the receiving optics, R is the range from the scattering species to the receiving optics, and the other symbols have the same meaning as previously mentioned. A uniform distribution of the scattering species has been assumed and the extinction between the sample and the collection optics has been assumed to be negligible.

C. P_s for Raman Sidescatter Measurements. For a spectrometer observing scattered light in a direction perpendicular to that of the radiation incident on the sample

$$P_s(\text{SS}) = P_o N\left(\frac{d\sigma}{d\Omega}\right) L\eta_o\eta_d \quad (6)$$

where the symbols have been defined previously. Note that L for such an experiment is likely to be on the order of one centimeter for sidescatter, whereas for backscatter measurements, $L = c\tau/2$ is on the order of 3 m for a 20 nsec pulse.

D. P_s for CARS. The general relationship for the anti-Stokes power, P_3, generated in a three-wave mixing process due to tightly focused beams is given as:[13, 17]

$$P_3 \cong \left(\frac{\pi}{\lambda}\right)^2\left(\frac{4\pi^2\omega_3}{c^2}\right)^2|3\chi|^2P_1^2P_2 = K|\chi|^2P_1^2P_2 \quad (7)$$

where

$$K = \left(\frac{\pi}{\lambda}\right)^2\left(\frac{12\pi^2\omega_3}{c^2}\right)^2, \quad (8)$$

λ is an average wavelength for the three beams involved, ω_3 is the angular frequency of the anti-Stokes signal, χ is the third-order nonlinear susceptibility coefficient, and P_1 and P_2 are the powers of the pump laser and the laser at the Stokes frequency, respectively.

As has been pointed out[16] the susceptibility for a given material or mixture is composed of a background susceptibility, χ_{NR}, which is relatively independent of the frequencies used in the experiment, and a resonant χ, χ_R, given by

$$\chi_R \cong \frac{\chi_P\gamma}{2\omega - i\gamma} \quad (9)$$

where χ_P is the peak value of χ_R, γ is the full width at half-maximum, as before, and $\omega = \omega_1 - \omega_2 - \omega_r$ is the difference between the resonance frequency, ω_r, and the difference frequency, $\omega_1 - \omega_2$, between the pump beam and the Stokes beam.

For weak signals in which $\chi_P \ll \chi_{NR}$,

$$|\chi| = \left|\chi_{NR} + \frac{\chi_P\gamma}{2\omega - i\gamma}\right| \cong \chi_{NR} + \frac{2\chi_P\gamma\omega}{4\omega^2 + \gamma^2} \quad (10)$$

The magnitudes of χ at its extrema are equal to $\chi_{NR} \pm \chi_P/2$. For $\chi_P \ll \chi_{NR}$, as would be the case for a weak resonance or for a dilute mixture,

$$\left(\chi_{NR} + \frac{\chi_P}{2}\right)^2 = \chi_{NR}^2 + \chi_{NR}\chi_P. \quad (11)$$

When considering a dilute component in a mixture or a weak resonance in a sample the deviation of the square of the susceptibility from $|\chi_{NR}|^2$ (i.e., $\chi_{NR}\chi_P$) is considered to result in the signal for which the S/N is to be computed. This is in contrast to the relationships developed for Raman scattering (Eqs. (5) and (6)) in which every photon is considered to contribute to the signal. This definition is necessary for CARS because fluctuations in the magnitude of the coherent scattered beam due to χ_{NR} contribute to fluctuations in the determination of χ_P. The peak deviation in the power due to the resonance is thus obtained from Eqs. (7) and (8):

$$P_s(\text{CARS}) = K\chi_{NR}\chi_P P_1^2P_2\eta_c\eta_o\eta_d \quad (12)$$

where η_c is the observed conversion efficiency for a given CARS experiment relative to the theoretical value given in Eq. 7. With careful experimental techniques, Taran[25] has observed values of η_c equal to 0.01 to 0.1[25] whereas poor beam quality, saturation effects, or turbulence can cause η_c to be much less.

E. P_{N1} for Amplitude Fluctuations in Laser Beam. One of the most common sources of noise in an experiment which must determine a difference signal between

two large background signals is the fluctuation in the magnitude of the background signal. If pulsed monochromatic lasers are used, the standard deviation of the power in a successive train of pulses is equal to the noise power, given by

$$P_{N1} = \epsilon_P P_r \tag{13}$$

where ϵ_P is the relative standard deviation of the light source and P_r is the power which is converted into signal at the detector. For an absorption measurement,

$$P_r(\text{ABS}) \cong P_o \eta_o \eta_d. \tag{14}$$

For a Raman experiment, the magnitude of the signal is likely to be so weak that other noise sources such as shot noise dominate. For a CARS experiment, the magnitude of the background signal due to χ_{NR} will fluctuate. For the case in which both P_1 and P_2 fluctuate with a relative standard deviation equal to ϵ_P, the noise power in the background signal due to χ_{NR} is given by obtaining an approximate standard deviation using Eq. 7:

$$P_{N1}(\text{CARS}) \cong 3\,\epsilon_P K |\chi_{NR}|^2 P_1^2 P_2 \eta_c \eta_o \eta_d. \tag{15}$$

F. P_{N2} for Shot Noise Due to Signal. Due to the corpuscular nature of electromagnetic radiation, n photons will have a standard deviation equal to approximately $\sqrt{n}$. This is referred to as shot noise in CW experiments. It is a significant source of noise for low level signals such as those in Raman scattering and low pressure CARS experiments. For pulsed signals

$$P_{N2}^2 = \frac{P_r h\nu}{\tau} \tag{16}$$

where h is Planck's constant, ν is the radiation frequency, and τ is the duration of the pulse. Shot noise due to background radiation is a common limitation to detectors in the infrared. The performance of a given detector is frequently rated with a detectivity D^*. Such noise sources are usually negligible for visible radiation and are hence not considered here. For high power infrared signals the noise source is typically due to amplitude fluctuations.

G. S/N for Absorption. Assuming the dominant noise source in an absorption experiment to be due to the amplitude fluctuations in the radiation source, combining Eqs. (4) and (13).

$$(\text{S/N})_{\text{ABS}} = \frac{1}{\epsilon_P}\left(\frac{2}{\pi}\frac{PSL}{\gamma}\right). \tag{17}$$

H. S/N for Raman Scattering. For Raman scattering experiments, a predominant source of noise is the shot noise due to the received signal. Other sources of noise include dark current in the detector and stray radiation. Conventionally, in discussing the ultimate limits of Raman scattering, the shot noise in the received signal is considered only.[24] With the use of Eq. (16), recognizing that ideally P_r is equal to P_s,

$$(\text{S/N})_{\text{RAMAN}} = \left(\frac{P_s \tau}{h\nu}\right)^{1/2}. \tag{18}$$

For a backscatter experiment, Eq. (5) is used for P_s, whereas for a sidescatter experiment, Eq. (6) is used.

I. S/N for CARS. The source of noise in a CARS experiment depends critically on the relative magnitude of the signal to the amplitude fluctuations in the laser beams. In general, if the magnitude of the background signal due to χ_{NR} is intense, the major source of noise will be due to the fluctuation of the laser beams. If the magnitude of the anti-Stokes beam is very weak, the major source of noise will be due to photon statistics. Relationships may be readily written down for each of these extremes.

For the case in which the noise source is dominated by the fluctuation in background signal the signal/noise ratio is given by Eqs. (12) and (15):

$$(\text{S/N})_{\text{CARS}} \cong \frac{\chi_P}{3\,\epsilon_P \chi_{NR}}. \tag{19}$$

For the case in which the noise source is due to photon statistics of low light levels, Eq. 18 is used with P_s given as P_3 of Eq. 7, modified for the efficiencies of each process:

$$(\text{S/N})_{\text{CARS}} = \left(\frac{K\chi_P^2 P_1^2 P_2 \eta_c \eta_o \eta_d \tau}{h\nu}\right)^{1/2}. \tag{20}$$

II. ASSUMED PARAMETERS

In order to make a comparison of these methods, a reasonable set of experimental parameters must be assumed. Applications of interest in which noise is likely to significantly affect the measurements include (1) trace analysis of pollutants in gases, (2) analytical and diagnostic examination of combustion processes at 1 atm, and (3) the examination of gases at pressures below 1 atm, including plasmas and the gain region of laser cavities.

A. Sample Length. For absorption spectra, increased length gives increased signal/noise ratio (Eq. (17)) until atmospheric extinction due to scattering or other absorptions begin to reduce or interfere with the signal level. With long path lengths in the open atmosphere, turbulence introduces additional sources of noise. The technique of fast derivative spectroscopy has been used[26] to reduce the noise introduced by turbulence. A path length of 1.0 km is a reasonable path length in experiments of this type. An alternative experimental arrangement may be envisioned in which a multi-pass cell is utilized with a sample at reduced pressure in order to reduce the linewidth. A total effective length of 10 m may be estimated for such an experiment.

For Raman backscatter experiments the effective length is $c\tau/2$[24] where c is the speed of light and τ is the duration of the pulse. A typical minimum value for the scattering range, R, is about 3 m.[27]

For examination of small scale combustion phenomena in the laboratory, Raman scattering perpendicular to the direction of the exciting radiation is typically used. In a typical spectrometer the scattered radiation from approximately a 1 cm length is collected and focused onto a slit.

In the CARS process, the conversion to anti-Stokes photons is typically within several confocal parameters of the focused laser beams. This varies from millime-

ters to several centimeters, depending on the choice of focal length of the lens employed.

B. Linewidths. The linewidth due to a gaseous sample at 1 atm is typically broadened by collisions. For carbon monoxide the width of a single rotational-vibrational transition in the infrared is approximately 0.1 cm^{-1}.[26] Linewidths of H_2, N_2, and O_2 observed by Raman scattering are given in Table I.[15, 28]

At reduced pressures, the width of a collision-broadened line decreases to the point at which Doppler broadening becomes the dominant mechanism. The collision broadened linewidth is given by[29]

$$\gamma \text{ (collision)} \, \alpha \, \frac{P}{T^{1/2}}. \tag{21}$$

According to this equation the width of a collision-broadened line appears to decrease as the temperature is increased and the pressure is held constant.

The Doppler width of an absorption line is given as

$$\gamma \text{ (Doppler)} = \left[\frac{8(\ln 2)kT}{m\lambda_v^2}\right]^{1/2} \tag{22}$$

where m is the molecular mass and λ_v the vibrational spectral wavelength. The respective relationships for Raman scattering[30,31] and for CARS[32] give Doppler widths which are slightly different than those for absorption. The Doppler widths used for the calculations are those predicted by Eq. (22). Using these alternative expressions does not alter the results significantly.

C. Amplitude Fluctuations. For both absorption spectra and CARS in relatively high pressure samples, the amplitude fluctuation in the intensity of the probe beam(s) is likely to represent the dominant source of noise. By averaging over n pulses, it is well known that the signal/noise ratio increases in proportion to the square root of n. High repetition rates are thus desirable to reduce noise due to this effect in a reasonable period of time.

Presently typical MW pulsed lasers have power fluctuations on the order of 5%. Note that, by Eq. (12), this means approximately a 15% fluctuation in the magnitude of the anti-Stokes signal. This represents a major source of noise, especially when the background level due to χ_{NR} is comparable with or greater than the peak value, χ_p, due to the resonance. In several instances[11,32] a second reference cell has been used such that the ratio between the anti-Stokes signal in the sample to that in the reference cell is obtained. This appears to improve the signal/noise levels to a certain extent. With a careful design, Moya *et al.*[16] report a fluctuation of 33% in the magnitude of the anti-Stokes signal (corresponding to a value for ϵ_p of 0.11). An obvious limit to the degree of cancellation which may be achieved is the nonlinearity of the electronics utilized to take the ratio. Instrumental nonlinearities are typically quoted to be on the order of 0.1%.

Throughout all of the calculations a value of ϵ_p was chosen to be 0.01. This is somewhat on the optimistic side of performance figures which have thus far been achieved by CARS, but somewhat pessimistic relative to the limit represented by electronic nonlinearities. It should be noted that any sample turbulence or inhomogeneity in the laser beams used for CARS represents a possible source of incoherent fluctuation of the CARS signal relative to the reference signal.

D. Spectral Envelope Calcuations. The value of χ_R for a single vibrational resonance has been given previously:[13,17]

$$\chi_R = \frac{2Nc^4}{3(\hbar\omega_2)^4}\left(\frac{d\sigma}{d\Omega}\right)\frac{\omega_v\Delta}{\omega_v^2 - (\omega_1 - \omega_2)^2 - i\gamma(\omega_1 - \omega_2)}. \tag{23}$$

Here, N is the number density, ω_1 and ω_2 are the angular frequencies of the pump laser and the Stokes frequency, respectively, ω_v is the angular frequency of the spectral transition and Δ is the relative population difference between the two vibrational levels. In the absence of saturation, Δ is a number close to unity.

The magnitude of $d\sigma/d\Omega$ has been tabulated for various molecules[13] and values are reproduced here for several species (Table I). It must be emphasized that the value tabulated is the Raman differential cross-section for the entire Q-branch spectrum. In order to estimate the value of χ_R for the spectral envelope in which the rotational transitions are resolved, the value of $d\sigma/d\Omega$ must be partitioned among the various rotational transitions. Taking this into account, the expression for χ_R becomes

$$\chi_R = \frac{2Nc^4}{3\hbar\omega_2^4}\left(\frac{d\sigma}{d\Omega}\right) \cdot \frac{\Delta}{Q}\sum_J \frac{g_J(2J+1)e^{-\frac{BJ(J+1)}{kT}}\omega_{v,J}}{\omega_{v,J}^2 - (\omega_1 - \omega_2)^2 - i\gamma(\omega_1 - \omega_2)} \tag{24}$$

where g_J is the statistical weight for level J due to the nuclear spin (for homonuclear diatomic molecules),

$$\omega_{v,J} = \omega_e - 2\omega_e x_e(v+1) - \alpha_e J(J+1), \tag{25}$$

ω_e is the harmonic vibrational frequency, x_e is the

TABLE I. Parameters used to calculate the limiting detectivity.

	H_2	N_2	O_2	CO	Ref.
Vibrational frequency, $1/\lambda_v$ (cm^{-1})	4155	2331	1556	2143	
Integrated absolute coefficient S (cm^{-2} atm^{-1})	···	···	···	9.98	23
$(d\sigma/d\Omega)/(d\sigma/d\Omega)_{N_2}$[a]	3.3	1.0	1.2	1.2	13
$\gamma(T = 300°K, P = 1$ atm) (cm^{-1})	0.03	0.14	0.16	0.15	28, 16
$\gamma(T = 1500°K, P = 1$ atm) (cm^{-1})	0.07	0.06	0.07	0.07	
$\gamma(T = 300°K$, Doppler broadened) (cm^{-1})	0.036	0.0055	0.0034	0.0050	
$\chi_p(T = 300°K, P = 1$ atm) ($\times 10^{16}$ cm^3/erg)	98.	2.4	2.6	2.6	
$\chi_p(T = 1500°K, P = 1$ atm) ($\times 10^{16}$ cm^3/erg)	4.4	0.32	0.35	0.27	

[a] $(d\sigma/d\Omega)_{N_2} = 4.4 \times 10^{-31}$ cm^2/sr[13]. Note also that $d\sigma/d\Omega$ is quoted for the entire spectral envelope.

Other parameters assumed:

L	= 1.0 km (absorption)
L	= 1.0 km (Raman sidescatter)
P_0	= P_1 = 5 MW
P_2	= 0.5 MW
R	= 3.0 m
ϵ_p	= 0.01
λ_0	= 532 nm for Raman scattering
λ_1	= 532 nm for CARS
τ	= 20 nsec
η_c	= 0.1
$(\eta_o\eta_d)$	= 0.1
χ_{NR}	($T = 300°K, P = 1$ atm) = 1.35×10^{-18} cm^3/erg (This value, taken from Rado[10] is lower (relative to χ_p for N_2) than other experiments indicate (Section II E).)
χ_{NR}	($T = 1500°K, P = 1$ atm) = 2.61×10^{-19} cm^3/erg.

anharmonic constant, α_e is the rotation-vibration interaction constant, and Q is the rotational partition function:

$$Q = \sum_J g_J(2J + 1)e^{-\frac{BJ(J+1)}{kT}}. \quad (26)$$

A computer routine was written to calculate the magnitude of χ_R vs $\omega_1 - \omega_2$. From this, peak values at the various resonances could be obtained.

E. Peak/Background Ratios for CARS. The signal/noise ratio depends critically on the ratio of the peak susceptibility, χ_P, to the background susceptibility, χ_{NR} (Eq. (19)). The value of χ_P may be estimated from the calculation of the spectral envelope by Eq. (24). The value of χ_{NR} has been measured for a number of gases by Rado.[10] A sample calculation involving nitrogen at 1 atm pressure serves to illustrate the difficulty in properly determining this ratio. By taking the results of the calculated χ_P and χ_{NR} from Rado,[10]

$$\left(\frac{\chi_P}{\chi_{NR}}\right)_{N_2} = 178. \quad (27)$$

It is to be noted that formulas used by Rado are inconsistent with the relationships utilized by Regnier *et al.*[13] by a factor of 3.[17]

A CARS spectrum of N_2 was recently reported[16] in which the interference between χ_{NR} and the resonant value of χ is observed. Such spectra may be utilized to determine values of χ_{NR} in solids and liquids.[7,32] For a single resonance, the difference between maximum and minimum conversion efficiency, $\delta\omega$, is given by[16]

$$\delta\omega = \gamma\left(1 + \frac{{\chi_P}^2}{4\chi_{NR}^2}\right)^{1/2} \quad (28)$$

where it has been assumed that the value of χ_{NR} is real.

The CARS spectrum of nitrogen consists of a number of resonances due to the rotational levels present. In the spectrum giving moderate resolution which has been reported,[16] the various lines in the Q-branch are unresolved. Treating the entire Q-branch as a single resonance, the separation between extrema is approximately 42 cm^{-1}. Combining this with the estimated linewidth of 1.8 cm^{-1} gives a value of

$$\left(\frac{\chi_P}{\chi_{NR}}\right)_{N_2} = 47. \quad (29)$$

This number is at variance with the ratio obtained by direct inspection, equal to the magnitude of the apparent peak value relative to the background. The value obtained by this method is

$$\left(\frac{\chi_P}{\chi_{NR}}\right)_{N_2} = 73. \quad (30)$$

The discrepancy between Eqs. (29) and (30) is due to the fact that a finite laser line width was utilized, along with the approximation that the entire Q-branch was treated as a single resonance. The discrepancy between 29 and 30 with 27 simply appears to represent experimental error in the determination of the absolute value of χ_{NR}.

III. STATISTICAL CONSIDERATIONS

A. Uncertainty in Determination of χ_P. The uncertainty in which the intensity of a given spectral transition may be determined, given an assumed signal/noise ratio, may be estimated by ordinary statistical methods. Typically a spectral envelope is observed while scanning the probe frequency over the resonance frequency. If the only variable treated in a least squares analysis is the intensity of the resonance (or if this parameter is uncorrelated with other variables such as linewidth, baseline, etc.) then the standard deviation in the determination of χ_P, σ_P, is given by[33]

$$\frac{1}{{\sigma_P}^2} = \sum_i \frac{1}{{\sigma_i}^2} \quad (31)$$

where σ_i is the standard deviation in the determination of σ_P from the ith observation (or the ith pulse in the case of information obtained from pulsed lasers).

The magnitude of σ_i is not necessarily determined in the same way for different experiments. For a CARS experiment in which the amplitude jitter of the background represents the major source of noise and in which the resonance is a small fraction of the background, the uncertainty in the amplitude of each pulse is approximately a constant, σ_M, as the frequencies are scanned over a spectrum. In this case,

$$\sigma_i = \sigma_M\left(\frac{\partial \chi_P}{\partial G(\omega_i, J, T)}\right) \quad (32)$$

where $G(\omega_i, J, T)$ is the intensity of the spectral envelope at $\omega_1 - \omega_2 - \omega_P = \omega_i$ due to rotational quantum number J, at temperature T. The standard deviation in χ_P is thus

$$\frac{1}{{\sigma_P}^2} = \frac{1}{{\sigma_M}^2}\sum_i\left(\frac{\partial G(\omega_i, J, T)}{\partial \chi_P}\right)^2. \quad (33)$$

For a Lorentzian line shape assuming a single resonance given by

$$\chi = \chi_{NR} + \frac{\chi_P\gamma}{2\omega + i\gamma} \quad (34)$$

in which $\omega = \omega_1 - \omega_2$, the CARS signal due to a resonance much weaker than the magnitude of the background is given approximately as

$$G(\omega_i, J, T) \cong K\left[\chi_{NR}^2 + \frac{4\chi_{NR}\chi_P\gamma\omega_i}{4{\omega_i}^2 + \gamma^2}\right]{P_1}^2P_2. \quad (35)$$

Substitution of this expression into Eq. 33 and evaluation of the resultant summation by integration gives

$$\sigma_P = \frac{\sigma_M}{K{P_1}^2P_2\chi_{NR}}\left(\frac{2\Delta\omega}{\pi\gamma}\right)^{1/2} \quad (36)$$

where $\Delta\omega$ is the spacing between successive ω_i as the probe frequency is swept over the resonance.

Using an argument similar to the development of Eq. (15), and recognizing σ_M as the standard deviation of $G(\omega_i, J, T)$ given by Eq. (35),

$$\sigma_M \cong 3\epsilon_P K\chi_{NR}^2{P_1}^2P_2. \quad (37)$$

Substituting this into Eq. (36) gives

$$\frac{\sigma_P}{\chi_P} = \frac{3\epsilon_P\chi_{NR}}{\chi_P}\left(\frac{2\Delta\omega}{\pi\gamma}\right)^{1/2} = \frac{1}{(S/N)_{peak}\sqrt{n}} \quad (38)$$

in which the signal/noise ratio at the peak of the resonance has been identified as

$$(S/N)_{peak} = \frac{\chi_P}{3\epsilon_P\chi_{NR}}$$

and the usual relationship has been introduced to account for the fact that the standard deviation on any quantity decreases with $n^{-1/2}$ for n measurements. By comparison in Eq. (38), effectively the number of pulses used to gather information is given by

$$n = \frac{\pi\gamma}{2\Delta\omega}. \quad (39)$$

A similar analysis for the standard deviation of the peak intensity of a Lorentzian line determined by Raman scattering gives the same result as that in Eq. (39).

B. Uncertainty in Determination of Temperature. As a practical application the degree of uncertainty in the rotational temperature of a flame may be estimated. This is accomplished by observing the intensities of the rotational lines present. The full least squares treatment requires a determination of the matrix of variances and covariances:[34,35]

$$\sigma_i^2(\mathbf{D}'\mathbf{D})^{-1}$$

where $\mathbf{D}$ is the matrix of derivatives and σ_i is the standard deviation for the observed signal. The diagonal elements of the matrix give the variance for the particular parameter determined. The parameters involving overall amplitude and temperature are not strongly correlated. Thus it is a fair approximation that the diagonal elements of the inverse matrix are the reciprocal of the diagonal elements in the product matrix $\mathbf{D}'\mathbf{D}$. With this approximation, the standard deviation for the temperature, σ_T, is approximated by

$$\frac{1}{\sigma_T^2} \cong \frac{1}{\sigma_M^2}\sum_J\left(\frac{\partial\, G(O, J, T)}{\partial\, T}\right)^2 \quad (40)$$

where $G(O, J, T)$ is the peak intensity of the spectral resonance with quantum number J and temperature T. In Eq. (40) it is also assumed that the standard deviation in the intensity of each resonance is the same.

Given the intensity of each rotational line (assuming $\chi_P \ll \chi_{NR}$) as

$$G(O, J, T)\alpha\frac{(2J+1)\exp[-BJ(J+1)/kT]}{Q} \quad (41)$$

then

$$\frac{\alpha G(O, J, T)}{\partial T} = \frac{G(O, J, T)[BJ(J+1) - \langle E\rangle]}{kT^2} \quad (42)$$

where

$$\langle E\rangle = \frac{1}{Q}\sum_J BJ(J+1)(2J+1)\exp[-BJ(J+1)/kT] \cong kT. \quad (43)$$

The additional relationship is introduced:

$$\sigma_M = G(O, J_{MAX}, T)\delta G(O, J_{MAX}, T) \quad (44)$$

where $G(O, J_{MAX}, T)$ is the magnitude of the most intense rotational line and $\delta G(O, J_{MAX}, T)$ is the relative uncertainty in the intensity of this line. Combining Eqs. (40), (42), (43), and (44),

$$\sigma_T^2 = \frac{T^2[\delta G(O, J_{MAX}, T)]^2}{\sum_J\left\{\frac{G(O, J, T)}{G(O, J_{MAX}, T)}\left[\frac{BJ(J+1)}{kT} - 1\right]\right\}^2} \quad (45)$$

giving an expression which may be readily evaluated for a specific example.

In particular, for carbon monoxide at 300°K,

$$\sigma_T^2 \cong (1/2)T\delta G(O, J_{MAX}, T)$$

whereas at 1500°K,

$$\sigma_T \cong (1/3)T\delta G(O, J_{MAX}, T).$$

Thus to know the temperature to within 10° at 1500°K requires a relative uncertainty in the amplitude of the strongest transition of 2%. If the signal/noise ratio is 10 on a pulse-to-pulse basis, 25 pulses will be required over the spectral width given by $\pi\gamma/2$. This represents the best one can do for an idealized example. Homonuclear diatomic molecules have nuclear spin effects which modify the above formulas somewhat. If the spectral lines overlap, as in the case with many diatomic species, the results of an analysis give a greater uncertainty than estimated here.

IV. RESULTS AND DISCUSSION

With the various sources of uncertainty categorized, the limiting capabilities of CARS may be compared with absorption and Raman sensitivities. Assuming a signal/noise ratio of unity and the parameters in Table I, discussed in Section II, the pressure for each gas is calculated and presented in Table II.

This isolated table is insufficient to relate other benefits which may be obtained with CARS. Other experi-

TABLE II. Calculated partial pressures of gas mixtures which give a specified S/N.

The values tabulated are $-\log_{20} P$ (atm). The first number in a given column corresponds to a S/N of unity, the second number corresponds to a S/N of 10. Example: For the CARS spectrum of N_2 at 300°K, 1 atm, S/N = 1 for a partial pressure of $10^{-3.8}$ atm, and S/N = 10 for a partial pressure of $10^{-2.8}$ atm.

	H_2	N_2	O_2	CO
1. Absorption (L = 1 km) (ambient pressure = 1 atm)	···	···	···	8.8/7.8
2. Absorption (L = 10 m) (γ = Doppler broadened)	···	···	···	9.1/8.1
3. Raman backscatter (T = 300°K)	6.3/4.3	6.0/4.0	6.1/4.1	6.1/4.1
4. Raman sidescatter (T = 300°K)	5.8/3.8	5.5/3.5	5.5/3.5	5.5/3.5
5. CARS (T = 300°K, ambient pressure = 1 atm)	5.4/4.4	3.8/2.8	3.8/2.8	3.8/2.8
6. CARS[a] (T = 300°K, reduced pressure, observed species is a major component)	8.3/6.3	8.0/6.0	8.3/6.3	8.0/6.0

[a] Assuming no saturation.

ments may be envisioned which require alternative considerations. The degradation of sensitivity of Raman scattering methods when the sample luminesces has been recognized for a long time. CARS does not degrade nearly as readily in luminescent samples, as has been demonstrated.[9] In addition, suppose, a high resolution spectrum were desired. For a Raman scattering experiment a monochrometer would be used with a resolution of approximately half of one linewidth. This requires rejecting a significant portion of the Raman scattered light. A CARS experiment, however, inherently gathers high resolution information if the spectral widths of the probe beams are significantly less than the resonance line width. Estimating signal/noise ratio for a high resolution spectrum (Table III) indicates some advantage to using CARS.

Given the statistical treatment of Section III, it is clear that in order to obtain a relatively low uncertainty in the amplitude of the signal, or to determine temperature, a significantly greater signal/noise ratio is required. Assuming that the dominant noise source for CARS is due to background from χ_{NR} and that the dominant line broadening mechanism is due to collision broadening (true for N_2, O_2, and CO at 1 atm) Eqs. (19), (21), and (23) give

$$(S/N)_{CARS} \propto \frac{P_{partial}}{P_{total}^2} \tag{46}$$

where $P_{partial}$ is the partial pressure of the gas undergoing observation in a medium having a total pressure of P_{total}. For Raman scattering, Eqs. (5) and (18) give

$$(S/N)_{RAMAN} \propto P_{partial}^{1/2}. \tag{47}$$

It should be noted that some confusion could exist in comparing CARS with Raman scattering because of the different manner in which the signal/noise ratio scales for each.

The results given in Table III indicate some advantage in utilizing CARS if a high signal/noise ratio is desired with a high resolution spectrum. In examining gases at higher temperature, CARS appears to offer additional advantages. As the temperature of a gas is increased at constant pressure, the number density decreases, the linewidth decreases, and the intensity of the strongest rotational transition decreases due to changing population. The combined result is seen to degrade the sensitivity of Raman scattering more rapidly than for CARS.

Finally, at reduced total pressures, the linewidths of N_2, O_2, and CO decrease. The background signal from χ_{NR} also decreases significantly. In the case where collision broadening remains the dominant line-broadening mechanism, assuming negligible overlap of adjacent lines, reducing the total pressure and the partial pressure equally actually increases the signal/noise ratio. Caution should be used in interpreting these calculated results at reduced pressure. The effects of saturation have been previously noted.[16] The power levels utilized to make the present calculation would inevitably lead to power saturation with short focal length lenses. The ultimate sensitivity at reduced pressures will depend critically on successful avoidance of the saturation effects.

TABLE III. Calculated partial pressures of gas mixtures which give a specified S/N.

The values tabulated are $-\log_{10} P$ (atm). The first number in a given column corresponds to S/N = 1, the second to S/N = 10 (as in Table II).

	Raman side scatter	CARS
H_2(T = 300°K, P_{tot} = 1 atm)	5.8/3.8	5.4/4.4
H_2 (high resolution, T = 300°K, P_{tot} = 1 atm)	5.5/3.5	5.4/4.4
H_2 (high resolution, T = 1500°K, P_{tot} = 1 atm)	4.5/2.5	4.8/3.8
H_2 (high resolution, T = 300°K, reduced pressure, H_2 major component)	5.5/3.5	8.3/6.3
CO (S/N = 1, T = 300°K, P_{tot} = 1 atm)	5.5/3.5	3.8/2.8
CO (high resolution, T = 300°K, P_{tot} = 1 atm)	4.3/2.3	3.8/2.8
CO (high resolution, T = 1500°K, P_{tot} = 1 atm)	3.3/1.3	3.5/2.5
CO (high resolution, T = 300°K, reduced pressure, CO major component)	4.3/2.3	8.0/6.0

V. BACKGROUND SUPPRESSION

The presence of an anti-Stokes signal due to the nonresonant background contribution to the nonlinear susceptibility clearly represents a limitation in the detection capability of CARS. A method has been proposed in which the background susceptibility may be partially cancelled.[36] This method utilizes three separate frequencies, ω_0, ω_1, and ω_2 to generate ω_3 from two separate components in the sample. Basically the out-of-phase generation of ω_3 while on the high frequency side of a strong resonance interferes with that generated by χ_{NR}. By adjusting the difference between ω_0 and ω_2 at the frequency of minimum signal, ω_1 may be swept to obtain a spectrum due to a second resonance with an apparent decrease in background signal.

In order to estimate the magnitude of the background signal which may be cancelled by this method, consider the values of χ' and χ'' which may occur for a single resonance. The susceptibility due to a resonance in the presence of background (see Eq. (10)) may be described as a circle on the complex plane (Fig. 1). From elementary geometry, the minimum value of χ, χ_{min}, is found to be

$$\chi_{min} = \left(\chi_{NR}^2 + \frac{\chi_{P2}^2}{4}\right)^{1/2} - \frac{\chi_{P2}}{2} \cong \chi_{NR}\left(\frac{\chi_{NR}}{\chi_{P2}}\right) \tag{48}$$

where the approximation is valid for $\chi_{P2} \gg \chi_{NR}$.

The signal/noise ratio under these conditions becomes (from Eq. (19)):

$$(S/N)_{SUPPRESSION}^{BACKGROUND} \cong \frac{\chi_P}{3\epsilon_P \chi_{min}} = \frac{\chi_P}{3\epsilon_P \chi_{NR}}\left(\frac{\chi_{P2}}{\chi_{NR}}\right). \tag{49}$$

The signal/noise ratio for a weak signal is thus expected to increase by the ratio χ_{P2}/χ_{NR} by using this background suppression technique. Some very strong resonances have been observed. Levenson *et al.*[2] have demonstrated an interference on the high-frequency side of a resonance in diamond which appears to give a decrease in the conversion efficiency by 2 orders of magnitude. This then could conceivably be used to increase the signal/noise ratio by one order of magnitude under the most favorable conditions. When considering the possibility of background suppression in

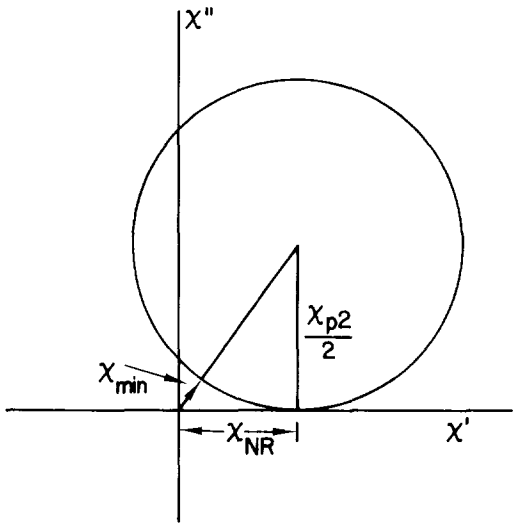

FIG. 1. χ' and χ'' plotted in the complex plane for a single resonance in the presence of background susceptibility χ_{NR}.

gases, hydrogen appears to have the strongest resonances reported thus far.[15] The spectra have an interference in which the background susceptibility decreases by a factor of nearly 20 in the pure gas. A 50% mixture of H_2 in another gas under examination could thus conceivably give an order of magnitude enhancement in the signal/noise ratio. For the examination of combustion phenomena, however, the presence of such a high concentration of hydrogen would most certainly represent a significant perturbation on the system under observation. With species such as N_2 or O_2, the susceptibility has been shown to drop an order of magnitude below background levels.[16] With an 80% concentration of N_2 in the sample, nearly an order of magnitude improvement might be expected.

A double CARS experiment may be performed in which the ratio of one CARS signal with a reference signal reduces the magnitude of the fluctuations due to laser amplitude jitter. With background suppression techniques, because of the additional sophistication required and the inherently lower power laser beams (three lasers rather than two), a reference cell represents additional experimental sophistication which may not yield the full improvement suggested by these calculations.

It should be pointed out that background suppression represents a possibility of attaining better signal/noise ratios than those tabulated. It is not yet a standard technique. Likewise, new methods have been developed with Raman scattering which increase the signal available. A multiple-pass Raman cell has been reported in which the Raman signal is enhanced by nearly 2 orders of magnitude,[37] resulting in an order of magnitude increase in signal/noise ratio.

VI. CONCLUSIONS

In the comparison of CARS with Raman scattering, it is evident that CARS offers several orders of magnitude improvement in the signal/noise ratio of simple gases at low pressure. The advantages of CARS in examining a luminescent sample have already been documented.[9] If the luminescence of a sample does not represent a difficulty, ordinary Raman scattering appears to offer somewhat greater ultimate sensitivity than CARS for samples at ambient pressures of 1 atm, except for the notable exception of hydrogen which has quite narrow linewidths.

The signal/noise ratio for CARS scales with pressure and temperature in quite a different manner than that for Raman scattering. This fact may introduce some confusion when comparing the two methods. Although it is true that Raman scattering offers greater ultimate sensitivity in terms of detectability of a minor species in a mixture at 1 atm pressure, CARS offers greater signal/noise ratios of high resolutions spectra.

A number of considerations must be taken into account when assessing the advantages of CARS relative to Raman scattering. It is hoped that the sample calculations illustrated herein allow a reasonable estimate of the present relative capabilities of the two methods.

ACKNOWLEDGMENTS

The authors wish to acknowledge helpful discussions with R. Byer, A. Harvey, and J. Nibler. This work was supported by the Office of Naval Research.

1. E. Yablonovitch, N. Bloembergen, and J. J. Wynne, Phys. Rev. **B3**, 2060 (1971).
2. M. D. Levenson, C. Flytzanis, and N. Bloembergen, Phys. Rev. **B6**, 3962 (1972).
3. J. J. Wynne, Phys. Rev. Letters **29**, 650 (1972).
4. M. D. Levenson and N. Bloembergen, J. Chem. Phys. **60**, 1323 (1974).
5. I. Chabay, G. K. Klauminzer, and B. S. Hudson, Appl. Phys. Letters **28**, 27 (1976).
6. I. Itzkan and D. A. Leonard, Appl. Phys. Letters **26**, 106 (1975).
7. M. D. Levenson and N. Bloembergen, Phys. Rev. **B10**, 4447 (1974).
8. R. F. Begley, A. B. Harvey, and R. L. Byer, Appl. Phys. Letters **25**, 387 (1974).
9. R. F. Begley, A. B. Harvey, R. L. Byer, and B. S. Hudson, J. Chem. Phys. **61**, 2466 (1974).
10. W. G. Rado, Appl. Phys. Letters **11**, 123 (1967).
11. P. R. Regnier and J-P. E. Taran, Appl. Phys. Letters **23**, 240 (1973).
12. P. R. Regnier and J-P. E. Taran, *Laser Raman Gas Diagnostics*, M. Lapp and C. M. Penney, Eds. (Plenum, New York, 1974).
13. P. R. Regnier, F. Moya, and J-P. E. Taran, AIAA J. **12**, 826 (1974).
14. J. J. Barrett and R. F. Begley, Appl. Phys. Letters **27**, 129 (1975).
15. F. Moya, S. A. J. Druet, and J-P. E. Taran, Opt. Commun. **13**, 169 (1975).
16. F. Moya, S. Druet, M. Pealat, and J-P. E. Taran, AIAA Paper No. 76-29, Presented at the AIAA 14th Aerospace Sciences Meeting and 12th Annual Meeting Aerospace 1976, Washington, DC, January 26–30, 1976.
17. W. M. Tolles, J. W. Nibler, J. R. McDonald, and A. B. Harvey, Appl. Spectrosc. in press.
18. C. J. Vear and P. J. Hendra, Chem. Commun. p. 381 (1972).
19. M. Lapp, L. M. Goldman, and C. M. Penney, Science **175**, 1112 (1972).
20. D. Hartley, M. Lapp, and D. Hardesty, Phys. Today, December, p. 37 (1975).
21. W. M. Arden, T. B. Hirschfeld, S. M. Klainer, and W. A. Mueller, Appl. Spectrosc. **28**, 554 (1974).
22. D. P. Aeschliman and R. E. Setchell, Appl. Spectrosc. **29**, 426 (1975).
23. K. G. P. Sulzmann, J. E. Lowder, and S. S. Penner, Combustion Flame **20**, 177 (1973).
24. R. L. Byer, Opt. Quant. E. **7**, 147 (1975).
25. J-P. E. Taran, Private communication.
26. R. T. Ku, E. D. Hinkley, and J. O. Sample, Appl. Opt. **14**, 854 (1975).
27. H. Inaba and T. Kobayashi, Opto-electronics **4**, 101 (1972).
28. W. H. Fletcher, Private communication.
29. S. S. Penner, *Quantitative Molecular Spectroscopy and Gas Emissivities* (Addison-Wesley, Reading, MA, 1959).
30. C. H. Townes, *Advances in Quantum Electronics* (Columbia University Press, New York, 1961).
31. W. R. L. Clements and B. P. Stoicheff, J. Mol. Spectrosc. **33**, 183 (1970).
32. R. L. Byer, Personal communication.
33. H. D. Young, *Statistical Treatment of Experimental Data* (McGraw-Hill, New York, 1962).
34. F. A Graybill, *An Introduction to Linear Statistical Models* (McGraw-Hill, New York, 1961).
35. J. A. Blackburn, *Spectral Analysis: Methods and Techniques* (Dekker, New York, 1970).
36. R. T. Lynch, Jr., S. D. Kramer, H. Lotem, and N. Bloembergen, Opt. Commun. **18**, 109 (1976).
37. R. A. Hill and D. L. Hartley, Appl. Opt. **13**, 186 (1974).